

# Exploring Increasing-Chord Paths and Trees

Yeganeh Bahoo\*

Stephane Durocher\*<sup>§</sup>

Sahar Mehrpour<sup>†</sup>

Debajyoti Mondal<sup>‡§</sup>

## Abstract

A straight-line drawing  $\Gamma$  of a graph  $G = (V, E)$  is a drawing of  $G$  in the Euclidean plane, where every vertex in  $G$  is mapped to a distinct point, and every edge in  $G$  is mapped to a straight line segment between their endpoints. A path  $P$  in  $\Gamma$  is called increasing-chord if for every four points (not necessarily vertices)  $a, b, c, d$  on  $P$  in this order, the Euclidean distance between  $b, c$  is at most the Euclidean distance between  $a, d$ . A spanning tree  $T$  rooted at some vertex  $r$  in  $\Gamma$  is called increasing-chord if  $T$  contains an increasing-chord path from  $r$  to every vertex in  $T$ . We prove that given a vertex  $r$  in a straight-line drawing  $\Gamma$ , it is NP-complete to decide whether  $\Gamma$  contains an increasing-chord spanning tree rooted at  $r$ , which answers a question posed by Mastakas and Symvonis [9]. We also shed light on the problem of finding an increasing-chord path between a pair of vertices in  $\Gamma$ , but the computational complexity question remains open.

## 1 Introduction

In 1995, Icking et al. [6] introduced the concept of a self-approaching curve. A curve is called *self-approaching* if for any three points  $a, b$  and  $c$  on the curve in this order,  $|bc| \leq |ac|$ , where  $|xy|$  denotes the Euclidean distance between  $x$  and  $y$ . A path  $P$  in a straight-line drawing  $\Gamma$  is called increasing-chord if for every four points (not necessarily vertices)  $a, b, c, d$  on  $P$  in this order, the inequality  $|bc| \leq |ad|$  holds.  $\Gamma$  is called an *increasing-chord drawing* if there exists an increasing-chord path between every pair of vertices in  $\Gamma$ .

Alamdari et al. [1] examined the problem of recognizing increasing-chord drawings, and the problem of constructing such a drawing on a given set of points. They showed that it is NP-hard to recognize increasing-chord drawings in  $\mathbb{R}^3$ , and asked whether it is also NP-hard in  $\mathbb{R}^2$ . They also proved that for every set of  $n$  points  $P$  in  $\mathbb{R}^2$ , one can construct an increasing-chord drawing  $\Gamma$  with  $O(n)$  vertices and edges, where  $P$  is a subset

of the vertices of  $\Gamma$ . In this case,  $\Gamma$  is called a *Steiner network of  $P$* , and the vertices of  $\Gamma$  that do not belong to  $P$  are called Steiner points. Dehkordi et al. [4] proved that if  $P$  is a convex point set, then one can construct an increasing-chord network with  $O(n \log n)$  edges, and without introducing any Steiner point. Mastakas and Symvonis [8] improved the  $O(n \log n)$  upper bound on edges to  $O(n)$  with at most one Steiner point. Nöllenburg et al. [11] examined the problem of computing increasing-chord drawings of given graphs. Recently, Bonichon et al. [3] showed that the existence of an angle-monotone path of width  $0 \leq \gamma < 180^\circ$  between a pair of vertices (in a straight-line drawing) can be decided in polynomial time, which is very interesting since angle-monotone paths of width  $\gamma \leq 90^\circ$  satisfy increasing chord property.

Nöllenburg et al. [10] showed that partitioning a plane graph drawing into a minimum number of increasing-chord components is NP-hard, which extends a result of Tan and Kermarrec [12]. They also proved that the problem remains NP-hard for trees, and gave polynomial-time algorithms in some restricted settings. Recently, Mastakas and Symvonis [9] showed that given a point set  $S$  and a point  $v \in S$ , one can compute a rooted minimum-cost spanning tree in polynomial time, where each point in  $S \setminus \{v\}$  is connected to  $v$  by a path that satisfies some monotonicity property. They also proved that the existence of a monotone rooted spanning tree in a given geometric graph can be decided in polynomial time, and asked whether the decision problem remains NP-hard also for increasing-chord or self-approaching properties.

## 2 Technical Background

Given a straight line segment  $l$ , the *slab of  $l$*  is an infinite region lying between a pair of parallel straight lines that are perpendicular to  $l$ , and pass through the endpoints of  $l$ . Let  $\Gamma$  be a straight-line drawing, and let  $P$  be a path in  $\Gamma$ . Then the *slabs of  $P$*  are the slabs of the line segments of  $P$ . We denote by  $\Psi(P)$  the arrangement of the slabs of  $P$ . Figure 1(a) illustrates a path  $P$ , where the slabs of  $P$  are shown in shaded regions. Let  $A$  be an arrangement of a set of straight lines such that no line in  $A$  is vertical. Then the *upper envelope of  $A$*  is a polygonal chain  $U(A)$  such that each point of  $U(A)$  belongs to some straight line of  $A$ , and they are visible from the point  $(0, +\infty)$ . The upper envelope of a set

\*Department of Computer Science, University of Manitoba, Winnipeg, Canada, {bahoo,durocher}@cs.umanitoba.ca

<sup>†</sup>School of Computing, University of Utah, Utah (UT), USA, mehrpour@cs.utah.edu

<sup>‡</sup>Cheriton School of Computer Science, University of Waterloo, Waterloo, Canada, dmondal@uwaterloo.ca

<sup>§</sup>Work of the author is supported in part by the Natural Sciences and Engineering Research Council of Canada (NSERC).

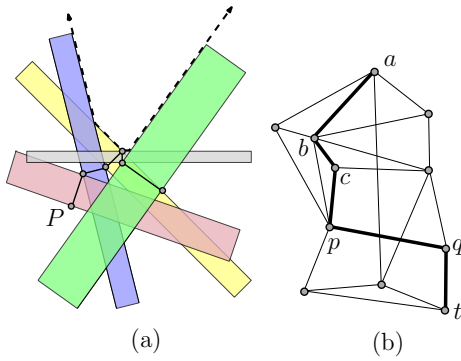


Figure 1: (a) Illustration for  $\Psi(P)$ , where the upper envelope is shown in dashed line. (b) An increasing-chord extension of  $a, b, \dots, p$  is shown in bold.

of slabs is the upper envelope of the arrangement of lines corresponding to the slab boundaries, as shown in dashed line in Figure 1(a). Let  $t$  be a vertex in  $\Gamma$  and let  $Q = (a, b, \dots, p)$  be an increasing-chord path in  $\Gamma$ . A path  $Q' = (a, b, \dots, p, \dots, t)$  in  $\Gamma$  is called an *increasing-chord extension* of  $Q$  if  $Q'$  is also an increasing-chord path, e.g., see Figure 1(b).

**Observation 1 (Icking et al. [7])** *A polygonal path  $P$  is increasing-chord if and only if for each point  $v$  on the path, the line perpendicular to  $P$  at  $v$  does not properly intersect  $P$  except possibly at  $v$ .*

A straightforward consequence of Observation 1 is that every polygonal chain which is both  $x$ - and  $y$ -monotone, is an increasing-chord path. We will use Observation 1 throughout the paper to verify whether a path is increasing-chord. Let  $v$  be a point in  $\mathbb{R}^2$ . By the *quadrants of  $v$*  we refer to the four regions determined by the vertical and horizontal lines through  $v$ .

### 3 Increasing-Chord Rooted Spanning Trees

In this section we prove the problem (IC-TREE) of computing a rooted increasing-chord spanning tree of a given straight-line drawing to be NP-hard.

**Theorem 1** *Given a vertex  $r$  in a straight-line drawing  $\Gamma$ , it is NP-complete to decide whether  $\Gamma$  admits an increasing-chord spanning tree rooted at  $r$ .*

We reduce the NP-complete problem 3-SAT [5] to IC-TREE. Let  $I = (X, C)$  be an instance of 3-SAT, where  $X$  and  $C$  are the set of variables and clauses. We construct a straight-line drawing  $\Gamma$  and choose a vertex  $r$  in  $\Gamma$  such that  $\Gamma$  contains an increasing-chord spanning tree rooted at  $r$  if and only if  $I$  admits a satisfying truth assignment. Here we give an outline of the hardness proof and describe the construction of  $\Gamma$ . A detailed reduction is given in the full version [2].

Assume that  $\alpha = |X|$ , and  $\beta = |C|$ . Let  $l_h$  be the line determined by the  $X$ -axis.  $\Gamma$  will contain  $O(\beta)$  points above  $l_h$ , one point  $t$  on  $l_h$ , and  $O(\alpha)$  points below  $l_h$ , as shown in Figures 2(a)–(b). Each clause  $c \in C$  with  $j$  literals, will correspond to a set of  $j + 1$  points above  $l_h$ , and we will refer to the point with the highest  $y$ -coordinate among these  $j + 1$  points as the *peak*  $t_c$  of  $c$ . Among the points below  $l_h$ , there are  $4\alpha$  points that correspond to the variables and their negations, and two other points, i.e.,  $s$  and  $r$ . In the reduction, the point  $t$  and the points below  $l_h$  altogether help to set the truth assignments of the variables.

We will first create a straight-line drawing  $H$  such that every increasing-chord path between  $r$  and  $t_c$ , where  $c \in C$ , passes through  $s$  and  $t$ . Consequently, any increasing-chord tree  $T$  rooted at  $r$  (not necessarily spanning), which spans the points  $t_c$ , must contain an increasing-chord path  $P = (r, s, \dots, t)$ . We will use this path to set the truth values of the variables.

The edges of  $H$  below  $l_h$  will create a set of thin slabs, and the upper envelope of these slabs will determine a convex chain  $W$  above  $l_h$ . Each line segment on  $W$  will correspond to a distinct variable, as shown in Figure 2(b). The points that correspond to the clauses will be positioned below these segments, and hence some of these points will be ‘inaccessible’ depending on the choice of the path  $P$ . These literal-points will ensure that for any clause  $c \in C$ , there exists an increasing-chord extension of  $P$  from  $t$  to  $t_c$  if and only if  $c$  is satisfied by the truth assignment determined by  $P$ .

By the above discussion,  $I$  admits a satisfying truth assignment if and only if there exists an increasing-chord tree  $T$  in  $H$  that connects the peaks to  $r$ . But  $H$  may still contain some vertices that do not belong to this tree. Therefore, we construct the final drawing  $\Gamma$  by adding some new paths to  $H$ , which will allow us to reach these remaining vertices from  $r$ . We now describe the construction in details.

**Construction of  $H$ :** We first construct an arrangement  $\mathcal{A}$  of  $2\alpha$  straight line segments. The endpoints of the  $i$ th line segment  $L_i$ , where  $1 \leq i \leq 2\alpha$ , are  $(0, i)$  and  $(2\alpha - i + 1, 0)$ . We now extend each  $L_i$  downward by scaling its length by a factor of  $(2\alpha + 1)$ , as shown in Figure 3(a). Later, the variable  $x_j$ , where  $1 \leq j \leq \alpha$ , and its negation will be represented using the lines  $L_{2j-1}$  and  $L_{2j}$ . Let  $l_v$  be a vertical line segment with endpoints  $(2\alpha + 1, 2\alpha)$  and  $(2\alpha + 1, -5\alpha^2)$ . Since the slope of a line in  $\mathcal{A}$  is in the interval  $[-2\alpha, -1/(2\alpha)]$ , each  $L_i$  intersects  $l_v$ . Since the coordinates of the endpoints of  $L_i$  and  $l_v$  are of size  $O(\alpha^2)$ , and all the intersection points can be represented using polynomial space.

By construction, the line segments of  $\mathcal{A}$  appear on  $U(\mathcal{A})$  in the order of the variables, i.e., the first two segments (from right) of  $U(\mathcal{A})$  correspond to  $x_1$  and  $\bar{x}_1$ , the next two segments correspond to  $x_2$  and  $\bar{x}_2$ , etc.

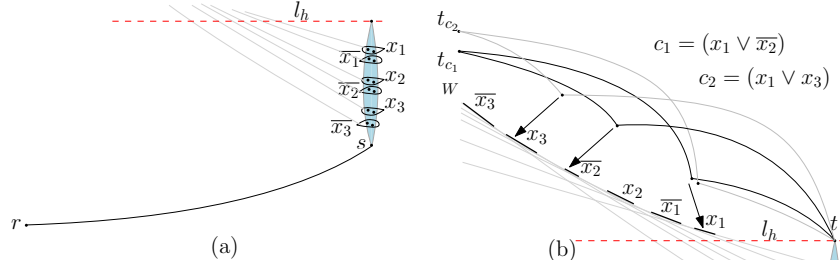


Figure 2: A schematic representation of  $\Gamma$ : (a) Points below  $l_h$ , (b) Points above  $l_h$ . The points that correspond to  $c_1$  and  $c_2$  are connected in paths of black, and gray, respectively. The slabs of the edges of  $H$  that determine the upper envelope are shown in gray straight lines. Each variable and its negation correspond to a pair of adjacent line segments on the upper envelope of the slabs. See the full version [2] for a better illustration.

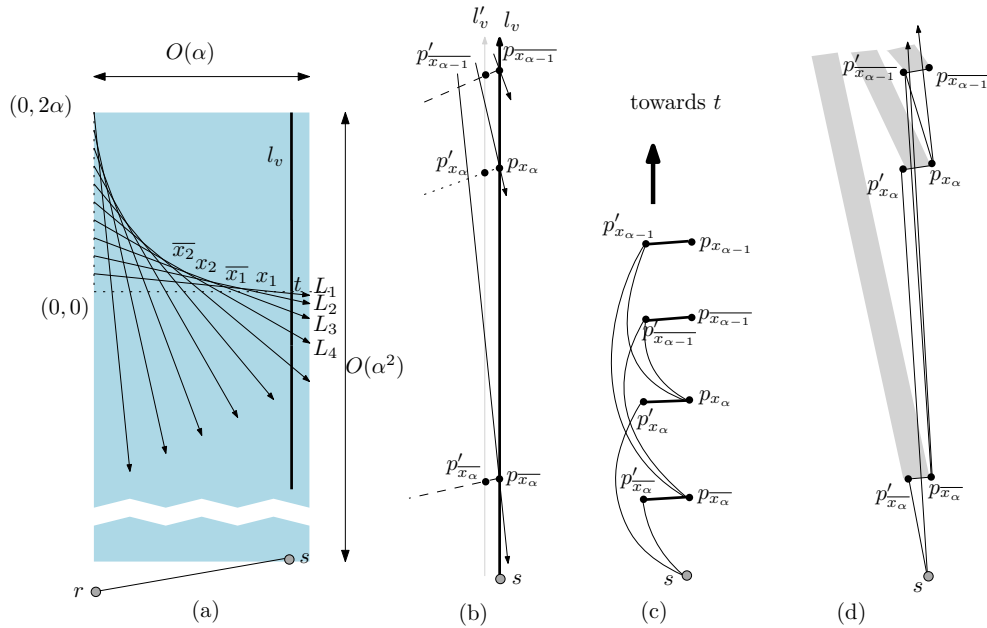


Figure 3: (a) Construction of  $\mathcal{A}$ . (b)–(c) Construction of the vertices and edges of  $H_b$ . (d) Illustration for the straight line segments of  $H_b$ , and the slabs corresponding to the needles.

**Variable Gadgets:** We denote the intersection point of  $l_h$  and  $l_v$  by  $t$ , and the endpoint  $(2\alpha + 1, -5\alpha^2)$  of  $l_v$  by  $s$ . We now create the points that correspond to the variables and their negations. Recall that  $L_{2j-1}$  and  $L_{2j}$  correspond to the variable  $x_j$  and its negation  $\bar{x}_j$ , respectively. Denote the intersection point of  $L_{2j-1}$  and  $l_v$  by  $p_{x_j}$ , and the intersection point of  $L_{2j}$  and  $l_v$  by  $p_{\bar{x}_j}$ , e.g., see Figure 3(b). For each  $p_{x_j}$  ( $p_{\bar{x}_j}$ ), we create a new point  $p'_{x_j}$  ( $p'_{\bar{x}_j}$ ) such that the straight line segment  $p_{x_j}p'_{x_j}$  ( $p_{\bar{x}_j}p'_{\bar{x}_j}$ ) is perpendicular to  $L_{2j-1}$  ( $L_{2j}$ ), as shown using the dotted (dashed) line in Figure 3(b). We may assume that all the points  $p'_{x_j}$  and  $p'_{\bar{x}_j}$  lie on a vertical line  $l'_v$ , where  $l'_v$  lies  $\varepsilon$  distance away to the left of  $l_v$ . The value of  $\varepsilon$  would be determined later. In the following we use the points  $p_{x_j}$ ,  $p_{\bar{x}_j}$ ,  $p'_{x_j}$  and  $p'_{\bar{x}_j}$  to create some polygonal paths from  $s$  to  $t$ .

For each  $j$  from 1 to  $\alpha$ , we draw the straight line segments  $p_{x_j}p'_{x_j}$  and  $p_{\bar{x}_j}p'_{\bar{x}_j}$ . Then for each  $k$ , where  $1 < k \leq \alpha$ , we make  $p_{x_k}$  and  $p_{\bar{x}_k}$  adjacent to both  $p'_{x_{k-1}}$  and  $p'_{\bar{x}_{k-1}}$ , e.g., see Figure 3(c). We then add the edges from  $s$  to  $p'_{x_\alpha}$  and  $p'_{\bar{x}_\alpha}$ , and finally, from  $t$  to  $p_{x_1}$  and  $p_{\bar{x}_1}$ . For each  $x_j$  ( $\bar{x}_j$ ), we refer to the segment  $p_{x_j}p'_{x_j}$  ( $p_{\bar{x}_j}p'_{\bar{x}_j}$ ) as the *needle* of  $x_j$  ( $\bar{x}_j$ ). Figure 3(c) illustrates the needles in bold. Let the resulting drawing be  $H_b$ .

Recall that  $l'_v$  is  $\varepsilon$  distance away to the left of  $l_v$ . We choose  $\varepsilon$  sufficiently small such that for each needle, its slab does not intersect any other needle in  $H_b$ , e.g., see Figure 3(d). The upper envelope of the slabs of all the straight line segments of  $H_b$  coincides with  $U(\mathcal{A})$ . Since the distance between any pair of points that we created on  $l_v$  is at least  $1/\alpha$  units, it suffices to choose  $\varepsilon = 1/\alpha^3$ . Note that the points  $p'_{x_j}$  and  $p'_{\bar{x}_j}$  can be represented in polynomial space using the endpoints of

$l'_v$  and the endpoints of the segments  $L_{2j-1}$  and  $L_{2j}$ . The proof of the following lemma is omitted (see [2]).

**Lemma 2** *Every increasing-chord path  $P$  that starts at  $s$  and ends at  $t$  must pass through exactly one point among  $p_{x_j}$  and  $p_{\bar{x}_j}$ , where  $1 \leq j \leq \alpha$ , and vice versa.*

We now place a point  $r$  on the  $y$ -axis sufficiently below  $H_b$ , e.g., at position  $(0, -\alpha^5)$ , such that the slab of the straight line segment  $rs$  does not intersect  $H_b$  (except at  $s$ ), and similarly, the slabs of the line segments of  $H_b$  do not intersect  $rs$ . Furthermore, the slab of  $rs$  does not intersect any segment  $L_j$ , and vice versa. We then add the point  $r$  and the segment  $rs$  to  $H_b$ . Let  $P$  be an increasing-chord path from  $r$  to  $t$ . The upper envelope of  $\Psi(P)$  is determined by the needles in  $P$ , which selects some segments from the convex chain  $W$ , e.g., see Figure 2(b). For each  $x_j$ ,  $P$  passes through exactly one point among  $p_{x_j}$  and  $p_{\bar{x}_j}$ . Therefore, for each variable  $x_j$ , either the slab of  $x_j$ , or the slab of  $\bar{x}_j$  appears on  $U(P)$ . Later, if  $P$  passes through point  $p_{x_j}$  ( $p_{\bar{x}_j}$ ), then we will set  $x_j$  to false (true). Since  $P$  is an increasing-chord path, by Lemma 2 it cannot pass through both  $p_{x_j}$  and  $p_{\bar{x}_j}$  simultaneously. Therefore, all the truth values will be set consistently.

**Clause Gadgets:** We now complete the construction of  $H$  by adding clause gadgets to  $H_b$ . For each clause  $c_i$ , where  $1 \leq i \leq \beta$ , we first create the peak point  $t_{c_i}$  at position  $(0, 2\alpha + i)$ . For each variable  $x_j$ , let  $\lambda_{x_j}$  be the interval of  $L_{2j-1}$  that appears on the upper envelope of  $\mathcal{A}$ . Similarly, let  $\lambda_{\bar{x}_j}$  be the interval of  $L_{2j}$  on the upper envelope of  $\mathcal{A}$ . For each  $c_i$ , we construct a point  $q_{x_j, c_i}$  ( $q_{\bar{x}_j, c_i}$ ) inside the cell of  $\mathcal{A}$  immediately below  $\lambda_{x_j}$  ( $\lambda_{\bar{x}_j}$ ). We will refer to these points as the *literal-points* of  $c_i$ . The full version [2] depicts these points in black squares. We assume that for each variable, the corresponding literal-points lie on the same location. One may perturb them to remove vertex overlaps. For each variable  $x \in c_i$ , we create a path  $(t, x, t_c)$ . In the reduction, if at least one of the literals of  $c_i$  is true, then we can take the corresponding path to connect  $t_c$  to  $t$ . Let the resulting drawing be  $H$ .

**Construction of  $\Gamma$ :** Let  $q$  be a literal-point in  $H$ . We now add an increasing-chord path  $P' = (r, a, q)$  to  $H$  in such a way that  $P'$  cannot be extended to any larger increasing-chord path in  $H$ . We place the point  $a$  at the intersection point of the horizontal line through  $q$  and the vertical line through  $r$ , the full version [2] contains the details. We refer to the point  $a$  as the *anchor* of  $q$ . By the construction of  $H$ , all the neighbors of  $q$  that have a higher  $y$ -coordinate than  $q$  lie in the top-left quadrant of  $q$ . Let  $q'$  be the first neighbor in the top-left quadrant of  $q$  in counter clockwise order. Since  $\angle aqq' < 90^\circ$ ,  $P'$  cannot be extended to any larger increasing-chord path  $(r, a, q, w)$  in  $H$ , where the  $y$ -coordinate of  $w$  is higher than  $q$ . On the other hand, every literal-point

$w$  in  $H$  with  $y$ -coordinate smaller than  $q$  intersects the slab of  $ra$ . Therefore,  $P'$  cannot be extended to any larger increasing-chord path.

For every literal-point  $q$  in  $H$ , we add such an increasing-chord path from  $t$  to  $q$ . To avoid edge overlaps, one can perturb the anchors such that the new paths remain increasing-chord and non-extensible to any larger increasing-chord paths. This completes the construction of  $\Gamma$ . We refer the reader to the full version [2] for the formal details of the reduction.

## 4 Increasing-Chord Paths

In this section we attempt to reduce 3-SAT to the problem of finding an increasing-chord path (IC-PATH) between a pair of vertices in a given straight-line drawing. We were unable to bound the coordinates of the drawing to a polynomial number of bits, and hence the computational complexity question of the problem remains open. We hope that the ideas we present here will be useful in future endeavors to settle the question.

Here we briefly describe the idea of the reduction. Given a 3-SAT instance  $I = (X, C)$ , the corresponding drawing  $\mathcal{D}$  for IC-PATH consists of straight-line drawings  $\mathcal{D}_{i-1}$ , where  $1 \leq i \leq \beta$ , e.g., see Figure 4(a). The drawing  $\mathcal{D}_{i-1}$  corresponds to the each clause  $c_i$ . We will refer to the bottommost (topmost) point of  $\mathcal{D}_{i-1}$  as  $t_{c_{i-1}}$  ( $t_{c_i}$ ). We will choose  $t_{c_0}$  and  $t_{c_\beta}$  to be the points  $t$  and  $t'$ , respectively, and show that  $I$  admits a satisfying truth assignment if and only if there exists an increasing-chord path  $P$  from  $t$  to  $t'$  that passes through every  $t_{c_i}$ . For every  $i$ , the subpath  $P_{i-1}$  of  $P$  between  $t_{c_{i-1}}$  and  $t_{c_i}$  will correspond to a set of truth values for all the variables in  $X$ . The most involved part is to show that the truth values determined by  $P_{i-1}$  and  $P_i$  are consistent. This consistency will be ensured by the construction of  $\mathcal{D}$ , i.e., the increasing-chord path  $P_{i-1}$  from  $t_{c_{i-1}}$  to  $t_{c_i}$  in  $\mathcal{D}_{i-1}$  will determine a set of slabs, which will force a unique increasing-chord path  $P_i$  in  $\mathcal{D}_i$  between  $t_{c_i}$  and  $t_{c_{i+1}}$  with the same truth values as determined by  $P_{i-1}$ .

**Construction of  $\mathcal{D}$ :** The construction of  $\mathcal{D}_{i-1}$  depends on an arrangement of lines  $\mathcal{A}^{i-1}$ . The construction of  $\mathcal{A}^0$  is the same as the construction of arrangement  $\mathcal{A}$ , which we described in Section 3. Figure 4(c) illustrates  $\mathcal{A}^0$  in dotted lines. For each variable  $x_j$ , where  $1 \leq j \leq \alpha$ , there exists an interval  $\lambda_{x_j}^0$  of  $L_{2j-1}$  on the upper envelope of  $\mathcal{A}^0$ . Similarly, for each  $\bar{x}_j$ , there exists an interval  $\lambda_{\bar{x}_j}^0$  of  $L_{2j}$  on the upper envelope of  $\mathcal{A}^0$ .

We now describe the construction of  $\mathcal{D}_0$ . Choose  $t_{c_0}$  ( $t_{c_1}$ ) to be the bottommost (topmost) point of  $\lambda_{x_1}^0$  ( $\lambda_{\bar{x}_\alpha}^0$ ). We then slightly shrink the intervals  $\lambda_{x_1}^0$  and  $\lambda_{\bar{x}_\alpha}^0$  such that  $t_{c_0}$  and  $t_{c_1}$  no longer belong to these segments. Assume that  $c_1$  contains  $\delta$  literals, where  $\delta \leq 3$ , and let  $\sigma_1, \dots, \sigma_{2^\delta-1}$  be the satisfying truth assignments for  $c_1$ . We construct a graph  $G_{c_1}$  that corresponds to these sat-

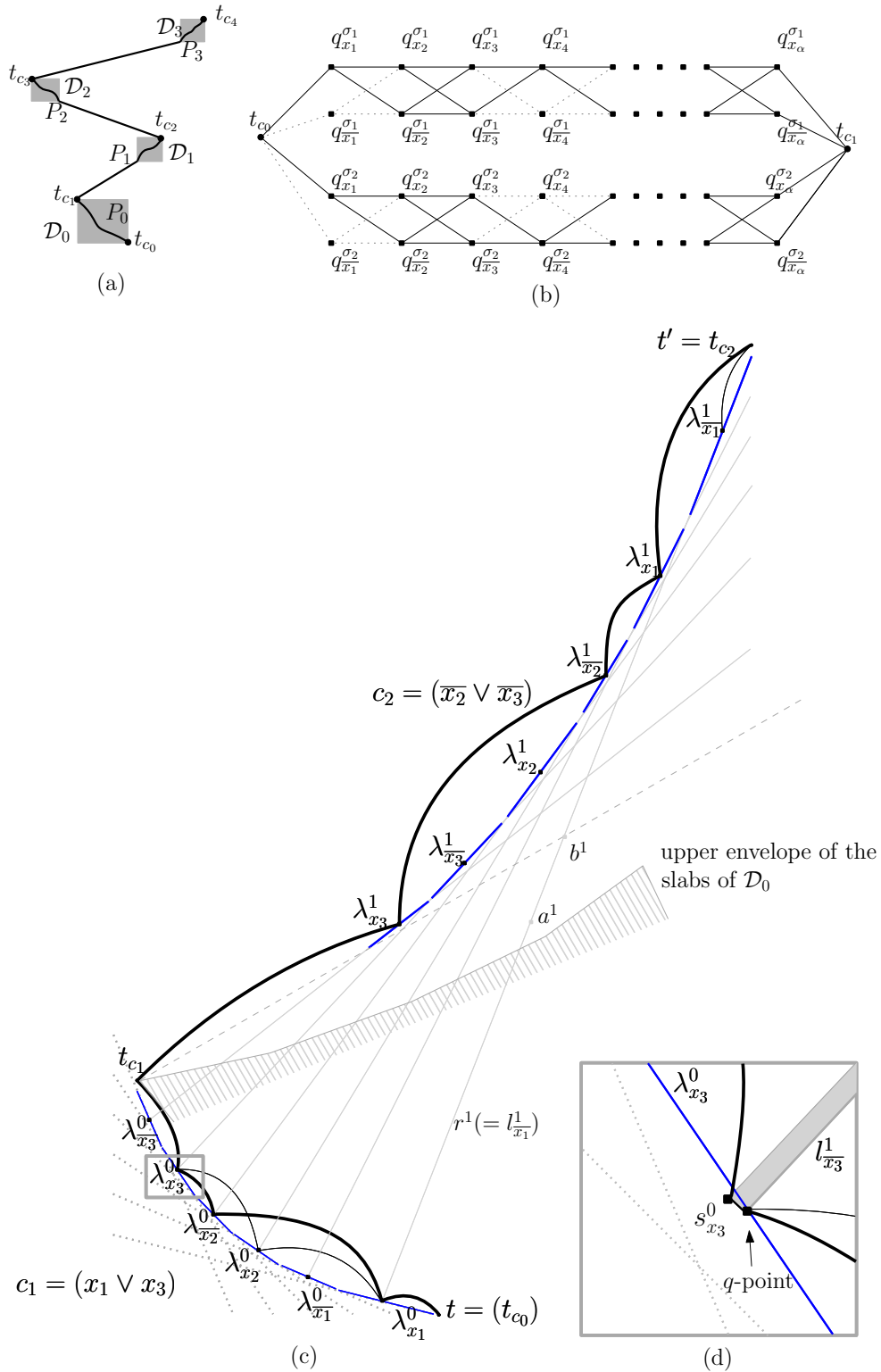


Figure 4: (a) Idea for the reduction. (b) The graph corresponding to the truth assignment satisfying  $c_1 = (x_1 \vee x_4)$ . Only the construction for the truth assignments  $\sigma_1 = \{x_1 = true, x_4 = true\}$  and  $\sigma_2 = \{x_1 = true, x_4 = false\}$  are shown. (c) A schematic representation for  $\mathcal{D}$ , where  $I = (x_1 \vee x_3) \wedge (\bar{x}_2 \vee \bar{x}_3)$ . An increasing-chord path is shown in bold, and the corresponding truth value assignment is:  $x_1 = true, x_2 = false, x_3 = true$ . (d) An  $s$ -segment.

isfying truth assignments, e.g., see Figure 4(b) and the full version [2] for formal details. The idea is to ensure that any path between  $t_{c_0}$  and  $t_{c_1}$  passes through exactly one point in  $\{q_{x_j}^{\sigma_k}, q_{\bar{x}_j}^{\sigma_k}\}$ , for each truth assignment  $\sigma_k$ , which will set the truth value of  $x_j$ . In  $\mathcal{D}_0$ , the point  $q_{x_j}^{\sigma_k}$  ( $q_{\bar{x}_j}^{\sigma_k}$ ) is chosen to be the midpoint of  $\lambda_{x_j}^{i-1}$  ( $\lambda_{\bar{x}_j}^{i-1}$ ). Later, we will refer to these points as  $q$ -points, e.g., see Figure 4(c). We may assume that for each  $x_j$ , the points  $q_{x_j}^{\sigma_k}$  lie at the same location. One may later perturb them to remove vertex overlaps.

By Observation 1, any  $y$ -monotone path  $P'$  between  $t_{c_0}$  and  $t_{c_1}$  must be an increasing-chord path. If  $P'$  passes through  $q_{x_j}^{\sigma}$ , then we set  $x_j$  to true. Otherwise,  $P'$  must pass through  $q_{\bar{x}_j}^{\sigma}$ , and we set  $x_j$  to false. In the following we replace each  $q$ -point by a small segment. The slabs of these segments will determine  $\mathcal{A}^1$ . Consider an upward ray  $r^1$  with positive slope starting at the  $q$ -point on  $\lambda_{x_1}$ , e.g., see Figure 4(c). Since all the edges that are currently in  $\mathcal{D}_0$  have negative slopes, we can choose a sufficiently large positive slope for  $r^1$  and a point  $a^1$  on  $r^1$  such that all the slabs of  $\mathcal{D}_0$  lie below  $a^1$ . We now find a point  $b^1$  above  $a^1$  on  $r^1$  with sufficiently large  $y$ -coordinate such that the slab of  $t_{c_1} b^1$  does not intersect the edges in  $\mathcal{D}_0$ . Let  $l_{\bar{x}_1}^1$  be the line determined by  $r^1$ . For each  $x_j$  and  $\bar{x}_j$  (except for  $j = 1$ ), we now construct the lines  $l_{\bar{x}_j}^1$  and  $l_{x_j}^1$  that pass through their corresponding  $q$ -points and intersect  $r^1$  above  $b^1$ . The lines  $l_{x_j}^1$  and  $l_{\bar{x}_j}^1$  determine the arrangement  $\mathcal{A}^1$ . Observe that one can construct these lines in the decreasing order of the  $x$ -coordinates of their  $q$ -points, and ensure that for each  $l_{x_j}^1$  ( $l_{\bar{x}_j}^1$ ), there exists an interval  $\lambda_{x_j}^1$  ( $\lambda_{\bar{x}_j}^1$ ) on the upper envelope of  $\mathcal{A}^1$ . Note that the correspondence is inverted, i.e., in  $\mathcal{A}^1$ ,  $\lambda_{\bar{x}_j}^1$  corresponds to  $\lambda_{x_j}^0$ , and  $\lambda_{x_j}^1$  corresponds to  $\lambda_{\bar{x}_j}^0$ .

For each  $j$ , we draw a small segment  $s_{x_j}^0$  ( $s_{\bar{x}_j}^0$ ) perpendicular to  $l_{x_j}^1$  ( $l_{\bar{x}_j}^1$ ) that passes through the  $q$ -point and lies to the left of  $q$ , e.g., see Figure 4(d). The construction of  $\mathcal{D}_i$ , where  $i > 1$ , is more involved. The upper envelope of  $\mathcal{A}^{i+1}$  is determined by the upper envelope of the slabs of the  $s$ -segments in  $\mathcal{D}_{i-1}$ . For each  $i$ , we construct the  $q$ -points and corresponding graph  $G_{c_i}$ . The full version [2] includes the formal details.

In the reduction we show that any increasing-chord path  $P$  from  $t$  to  $t'$  contains the points  $t_{c_i}$ . We set a variable  $x_j$  true or false depending on whether  $P$  passes through  $s_{x_j}^0$  or  $s_{\bar{x}_j}^0$ . The construction of  $\mathcal{D}$  imposes the constraint that if  $P$  passes through  $s_{x_j}^{i-1}$  ( $s_{\bar{x}_j}^{i-1}$ ), then it must pass through  $s_{x_j}^i$  ( $s_{\bar{x}_j}^i$ ). Hence the truth values in all the clauses are set consistently. By construction of  $G_{c_i}$ , any increasing-chord path between  $t_{c_{i-1}}$  to  $t_{c_i}$  determines a satisfying truth assignment for  $c_i$ . On the other hand, if  $I$  admits a satisfying truth assignment, then for each clause  $c_i$ , we choose the corresponding increasing-chord path  $P_i$  between  $t_{c_{i-1}}$  and  $t_{c_i}$ . The

union of all  $P_i$  yields the required increasing-chord path  $P$  from  $t$  to  $t'$ . The full version [2] presents the construction in details, and explains the challenges of encoding  $\mathcal{D}$  in a polynomial number of bits.

## 5 Open Problems

The most intriguing problem in this context is to settle the computational complexity of the increasing-chord path (IC-PATH) problem. Another interesting question is whether the problem IC-TREE remains NP-hard under the planarity constraint; a potential attempt to adapt our hardness reduction could be replacing the edge intersections by dummy vertices.

## References

- [1] S. Alamdari, T. M. Chan, E. Grant, A. Lubiw, and V. Pathak. Self-approaching graphs. In *Proc. of GD*, volume 7704 of *LNCS*, pages 260–271. Springer, 2013.
- [2] Y. Bahoo, S. Durocher, S. Mehrpour, and D. Mondal. Exploring increasing-chord paths and trees. *CoRR*, abs/1702.08380, 2017.
- [3] N. Bonichon, P. Bose, P. Carmi, I. Kostitsyna, A. Lubiw, and S. Verdonschot. Gabriel triangulations and angle-monotone graphs: Local routing and recognition. In *Proc. of GD*, volume 9801 of *LNCS*, pages 519–531. Springer, 2016.
- [4] H. R. Dehkordi, F. Frati, and J. Gudmundsson. Increasing-chord graphs on point sets. *Journal of Graph Algorithms and Applications*, 19(2):761–778, 2015.
- [5] M. R. Garey and D. S. Johnson. *Computers and intractability*. Freeman, San Francisco, 1979.
- [6] C. Icking and R. Klein. Searching for the kernel of a polygon - A competitive strategy. In *Proc. of SoCG*, pages 258–266. ACM, 1995.
- [7] C. Icking, R. Klein, and E. Langetepe. Self-approaching curves. In *Mathematical Proceedings of the Cambridge Philosophical Society*, volume 125, pages 441–453. Cambridge Univ Press, 1999.
- [8] K. Mastakas and A. Symvonis. On the construction of increasing-chord graphs on convex point sets. In *Proc. of IISA*, pages 1–6. IEEE, 2015.
- [9] K. Mastakas and A. Symvonis. Rooted uniform monotone minimum spanning trees. In *Proc. of CIAC*, volume 10236 of *LNCS*, pages 405–417. Springer, 2017.
- [10] M. Nöllenburg, R. Prutkin, and I. Rutter. Partitioning graph drawings and triangulated simple polygons into greedily routable regions. In *Proc. of ISAAC*, volume 9472 of *LNCS*, pages 637–649. Springer, 2015.
- [11] M. Nöllenburg, R. Prutkin, and I. Rutter. On self-approaching and increasing-chord drawings of 3-connected planar graphs. *JoCG*, 7(1):47–69, 2016.
- [12] G. Tan and A. Kermarrec. Greedy geographic routing in large-scale sensor networks: A minimum network decomposition approach. *IEEE/ACM Trans. Netw.*, 20(3):864–877, 2012.